IUHET-421
March 2000

SUSY Thresholds at a Muon Collider[1]

M. S. Berger

Physics Department, Indiana University, Bloomington, IN 47405

Abstract. One of the useful features of muon colliders is the naturally narrow spread in beam energies. Measurements of threshold cross sections then become a prime candidate for precision measurements of particle masses, widths, and couplings as well as determining particle spin. We describe the potential for measuring cross sections near threshold in supersymmetric theories.

INTRODUCTION

Muon colliders have negligible bremstrahlung and the beam energy can be measured very accurately by muon precession in the collider ring. Momentum spreads as low as $\Delta P/P = 0.003\%$ are thought to be achievable for a low-energy collider [1,2]. The beam energy could be determined with a precision of $\Delta E/E = 10^{-6}$ by measuring the time-dependent decay asymmetry resulting from the naturally polarized muons [3]. In addition, initial state radiation is smaller than at a electron-positron machine. These features make muon colliders especially useful for studying narrow resonances [4], and for measuring production cross sections near threshold where they change very rapidly [5–7]. However the cross sections are smaller near threshold, so high luminosity is required.

An important feature of cross sections near threshold is that they isolate the effects of the width and spin of the produced particle. The threshold cross section is a function of the particle's mass, decay width, spin, and coupling strength(s), and it (largely) factorizes near the threshold into an overall normalization and an energy-dependent part (profile).

The energy profile depends on the particle mass which dictates where in energy the cross section begins to rise; we say the cross section "turns on" near $2m$. The particle width and spin govern how fast the cross section rises with energy. The width is important because, on the one hand, we can think of the particle being produced and then subsequently decaying (the narrow width approximation); but on the other hand, one can more accurately view the process as one in which the

[1)] To appear in the *Proceedings of the 5th International Conference on Physics Potential and Development of $\mu^+\mu^-$ Colliders (MuMu99), San Francisco, CA, 15-17 December 1999.*

decay products are the final state and the decaying particle is a virtual particle. The rate the cross section rises depends then on the required "off-shellness" of this virtual particle.

As an example consider the cross section for $\mu^+\mu^- \to W^+W^-$ followed by the decay $W \to f\overline{f}'$ is given by [8]

$$\sigma(s) = B_{f_1\overline{f}_2} B_{f_3\overline{f}_4} \int_0^s ds_1 \rho(s_1) \int_0^{(\sqrt{s}-\sqrt{s_1})^2} ds_2 \rho(s_2) \sigma(s, s_1, s_2) \; , \tag{1}$$

where $\sigma(s, s_1, s_2)$ is the cross section for producing two virtural W bosons with invariant masses-squared of s_1 and s_2, and $B_{f_1\overline{f}_2}$ is the branching ratio for the decay $W \to f_1\overline{f}_2$. The weighting factor $\rho(s)$ arises from the W boson propagator and controls the rise of the cross section,

$$\rho(s) = \frac{1}{\pi} \frac{\sqrt{s}\Gamma(s)}{(s - M_W^2)^2 + M_W^2\Gamma(s)^2} \; . \tag{2}$$

The cross section $\sigma(s, s_1, s_2)$ is controlled by kinematics and angular momentum conservation for the region that $\rho(s_1)$ and $\rho(s_2)$ have significant support near $s_1, s_2 \approx M_W$. The couplings and radiative corrections are approximately energy-independent over this narrow range, and do not impact on the energy profile, but do affect the overall number of events expected.

CHARGINO PRODUCTION

Supersymmetric charginos can be pair produced at a muon collider. The two contributing Feynman diagrams for $\mu^+\mu^- \to \tilde{\chi}_1^+\tilde{\chi}_1^-$ is shown in Fig. 1. These two diagrams interfere desctructively over most of parameter space. The threshold measurement of the process $\mu^+\mu^- \to \tilde{\chi}_1^+\tilde{\chi}_1^-$ yields the following: a measurement of the $\tilde{\chi}_1^\pm$ mass, an indirect measurement of the $\tilde{\nu}_\mu$ mass, and a measurement of the overall normalization of the cross section.

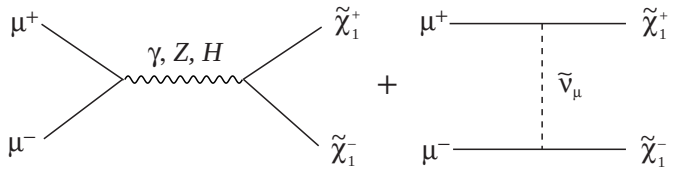

FIGURE 1. Feynman diagrams for chargino pair production.

The supersymmetric masses are known functions of the undetermined fundamental parameters of a given supersymmetric model, and are a window on the details of the supersymmetry breaking. For example the chargino mass matrix is

$$M_{\tilde{\chi}^{\pm}} = \begin{pmatrix} M_2 & \sqrt{2}M_W \sin\beta \\ \sqrt{2}M_W \cos\beta & -\mu \end{pmatrix}$$

The fundamental parameters of the supersymmetric model are the $SU(2)$ gaugino mass M_2, the supersymmetric Higgs mass μ, and the ratio of the vevs of the two Higgs doublets' vacuum expectation values, $\tan\beta = v_2/v_1$. The physically measured chargino masses $M_{\tilde{\chi}_1^{\pm}}$ and $M_{\tilde{\chi}_1^{\pm}}$ are obtained by diagonalizing this matrix. The masses and widths are complicated functions of fundamental parameters, but accurate measurements of the chargino masses constrain one to be on a slice through the parameter space of fundamental parameters.

The impact of different amounts of beam smearing is shown in Fig. 2. The narrow beam spread ($R = 0.1\%$, where R is the rms spread of the energy of a muon beam) of a muon collider can prove especially advantageous when the widths of the produced particles is substantially less than a GeV.

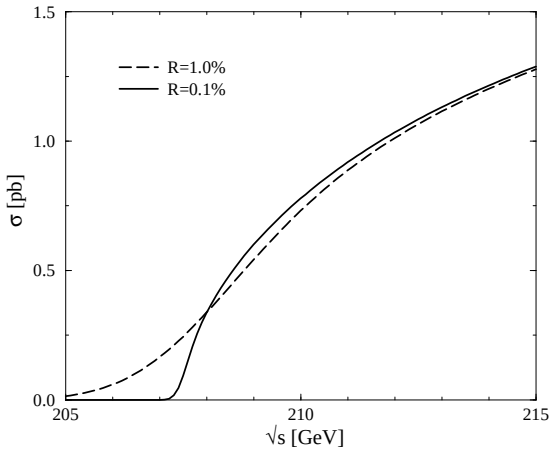

FIGURE 2. A muon beam with a narrow beam spread ($R = 0.1\%$) preserves the rapid rise in the chargino pair production threshold cross section. The threshold cross section convoluted with a beam with $R = 1.0\%$ is shown for comparison. The chargino parameters are $M_2 = 100$ GeV, $\tan\beta = 4$, and $\mu >> M_2$.

The chargino production cross section decreases with increasing chargino mass. Therefore the precision with which the mass can be measured is better at smaller values of the mass. Figure 3 shows the expect precision with 100 fb^{-1} integrated luminosity for sneutrino masses of 300 and 500 GeV. For a lighter sneutrino, for which the destructive interference between the s-channel and t-channel graphs is more severe, the precision obtained is reduced. The sneutrino mass can be measured to about 6 GeV accuracy for $m_{\tilde{\nu}} = 300$ GeV and to about 20 GeV accuracy for $m_{\tilde{\nu}} = 500$ GeV [9,10].

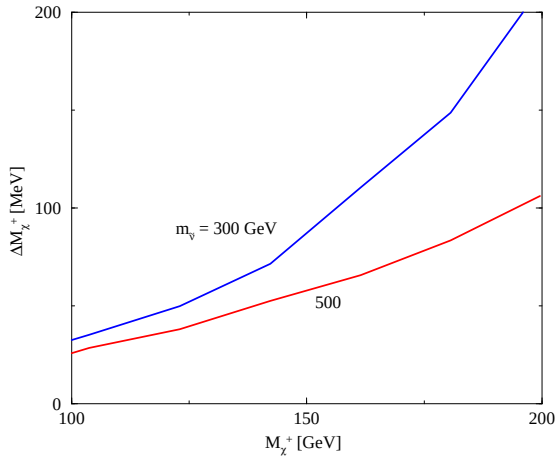

FIGURE 3. The 1σ precision obtainable in the chargino mass taking $m_{\tilde{\nu}} = 300$ and 500 GeV. The precision is better for *larger* sneutrino mass because the contribution from the t-channel sneutrino exchange diagram destructively interferes with the s-channel diagrams.

TOP SQUARK PRODUCTION

Scalar production is p-wave suppressed, so the threshold production cross section looks very different than for fermion pair production. For example one can compare top quark production to top squark production near threshold [11]. The top squark cross section shows a slow β^3 rise with little resonance structure [12]. The top squark threshold profile is very different that of the top quark. By measuring energy profile, one can determine the produced particle's spin. If the squarks are for some reason especially long-lived, then bounds states might be formed that would appear in the threshold cross section [7].

THRESHOLD HIGGS PRODUCTION

An accurate determination of the supersymmetric Higgs boson mass m_H can be obtained by measuring the threshold cross section for the Bjorken Higgs-strahlung process [13] $\mu^+\mu^- \to ZH$. The Higgs boson could be discovered in the ZH production mode by running the collider well above threshold. For $m_H < 2M_W$, as one expects in supersymmetric models, the primary decay channel is $b\overline{b}$, and most backgrounds can be eliminated by b-tagging.

The Higgs cross section near threshold is sensitive to the Higgs mass and width. In Fig. 4 the results [14,15] for a Higgs mass around 100 GeV are displayed. The solid curves show the $\Delta\chi^2 = 1$ contours for determining the Higgs mass versus $g^2_{ZZH}B(H \to b\overline{b})$, or versus Γ_H, by devoting 100/3 fb^{-1} to each of the c.m. energies $\sqrt{s} = M_Z + m_H + 0.5$ GeV, $\sqrt{s} = M_Z + m_H + 20$ GeV and $\sqrt{s} = M_Z + m_H - 2$ GeV

at a muon collider. included. The dashed curve shows the $\Delta\chi^2 = 1$ contour that results when Γ_H is negligibly small and 50 fb^{-1} is devoted to each of the c.m. energies $\sqrt{s} = m_H + M_Z + 0.5$ GeV and $\sqrt{s} = m_H + M_Z + 20$ GeV.

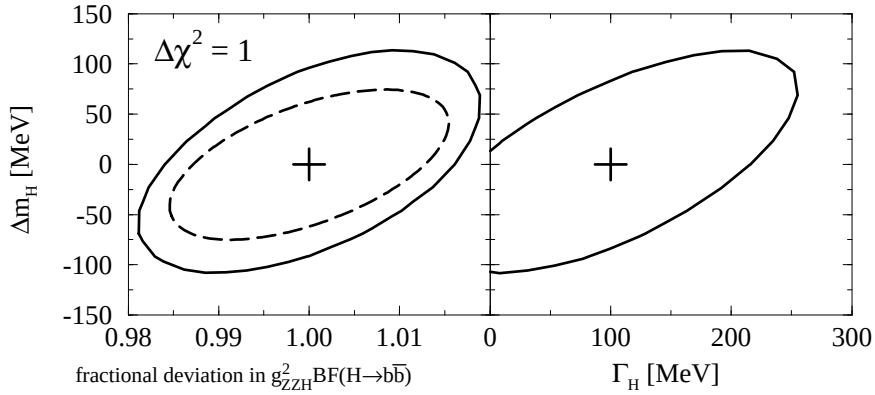

FIGURE 4. A simulatneous measurement of the Higgs mass and the overall rate $g^2_{ZZH}B(H \to b\bar{b})$ s shown on the left. A measurement of the Higgs width is shown on the right.

CONCLUSIONS

Muon colliders offer advantages for performing threshold cross section measurements: no beamstrahlung, small beam energy spread, reduced initial state radiation.

Precise measurements of particle masses and widths are possible, and the shape of the threshold cross section can be measured to determined the produced particle's spin.

ACKNOWLEDGEMENT

Work supported in part by the U.S. Department of Energy under Grant No. DE-FG02-95ER40661.

REFERENCES

1. C. M. Ankenbrandt, et al., *Phys. Rev. ST Accel. Beams* **2**, 081001 (1999), physics/9901022.
2. *Expression of Interest for R&D towards a Neutrino Factory Based on a Storage Ring and a Muon Collider*, physics/9911009.
3. R. Raja and A. Tollestrup, *Phys. Rev.* **D58**, 013005 (1998).

4. V. Barger, M. S. Berger, J. F. Gunion and T. Han, *Phys. Rep.* **286**, 1 (1997).
5. M. S. Berger, *The $t\bar{t}$ threshold at a muon collider*, hep-ph 9508209.
6. M. S. Berger, *Threshold Cross Section Measurements*, hep-ph 9802213.
7. CERN Report 99-02, eds. B. Autin, A. Blondel and J. Ellis.
8. T. Muta, R. Najima and S. Wakaizumi, Mod. Phys. Lett. **A1**, 203 (1986).
9. V. Barger, M. S. Berger and T. Han, *Phys. Rev.* **D59**, 071701 (1999).
10. M. S. Berger, *Precision Measurements of Threshold Chargino production*, hep-ph 9802265.
11. E. L. Berger, private communication.
12. W. Modritsch, *Nucl. Phys.* **B475**, 507 (1996).
13. J.D. Bjorken, *Proceedings of the Summer Institute on Particle Physics*, ed. M. Zipf (Stanford, 1976).
14. V. Barger, M. S. Berger and T. Han, *Phys. Rev.* **D56**, 1714 (1997).
15. M. S. Berger, *Precision W-Boson and Higgs Boson Mass Determinations at Muon Colliders*, hep-ph 9712474.